

Application of numerical methods to simulate the unsteady flow of lean liquor solution through a porous medium made up of porous ore particles

G.A. Sheikhzadeh⁽¹⁾, M.A. Mehrabian⁽¹⁾, S.H. Mansouri⁽¹⁾ and A. Sarrafi⁽²⁾

⁽¹⁾Mechanical Engineering Department, Shahid Bahonar University of Kerman, Kerman, IRAN
e-mail: ma_mehrabian@yahoo.com

⁽²⁾Chemical Engineering Department, Shahid Bahonar University of Kerman, Kerman, IRAN

SUMMARY

Unsaturated flow of liquid in a bed of uniform and spherical ore particles is studied numerically and experimentally. An unsteady and two-dimensional model is developed based on the mass conservation equations of liquid phase in the bed and in the particles. The model equations are solved using a fully implicit finite difference method giving the distribution of the degree of saturation in the particles and in the bed and the vertical velocity of flow in the bed, as well as, the effect of periodic infiltration on the above distributions. To calibrate the computational model, several column tests are performed using periodic infiltration of water on 40 cm high columns composed of ore having particles smaller than 25 mm. The numerical analysis shows that (a) the results obtained from numerical modelling under the same operating conditions as used for column tests, are in good agreement with those from experimental procedure, (b) the degree of saturation of the bed and the time required to reach steady state conditions depend on the inflow of water and intrinsic permeability of the bed and (c) the velocity fluctuations and the fluctuations of the degree of saturation in the bed depend on the inflow of water, period of infiltration, height and intrinsic permeability of the bed.

Key words: modelling, unsaturated liquid flow, heap leaching, porous media, column test.

1. INTRODUCTION

A porous medium is defined as a matrix of solid particles with interconnected void spaces. The solid matrix is considered rigid or having small deformations. The interconnection of the pores allows the flow of one or more fluids through the medium. In a natural porous medium, the shape and size of pores are irregular. Thus, in microscopic scale, the flow quantities (velocity, pressure, etc.) will be non-uniform, but for studying the flow in a porous medium, usually space-averaged quantities are used [1]. Heap leaching is one of the industrial processes in which fluid flows through a porous medium. In this process, unsaturated lean liquor solution flows in the ore bed together with chemical reactions [2]. The perception of fluid flow through ore heaps is described primarily from soil

mechanics, hydrogeology and chemical engineering theory supported by experimental information [3]. The solution in the bed is divided into two parts; the moving part that flows among the ore particles due to gravity and the stagnant part attached either to the pore walls of ore particles or to the particles external surfaces. The dissolution reactions of reactants occurred in the stagnant part, and the diffusion of reagent and species between these two parts is done by mass transfer mechanism [4]. One way of improving this operation is periodic irrigation of leaching solution on top of the ore heap. As a result of this, one can reach to a relatively constant concentration of dissolved species in the pregnant solution and enhance the performance of the recovery plant [5].

The understanding of hydrodynamics of liquid (leaching solution) is an important factor during heap

leaching operation. The purpose of this work is developing a computational model to analyze the flow of liquid through the bed of ore particles and the transport of liquid within the particles.

Martinez et al. [5] simulated the periodic infiltration of water in heap leaching based on mass conservation equation for liquid inside the bed as well as the liquid within the particles. They used the semi implicit finite difference technique (Crank Nicolson) to solve the set of discretized equations. Sheikhzadeh et al. [6] improved the Martinez et al. [5] computational model using a fully implicit finite difference technique [6]. Sheikhzadeh et al. used the same operating conditions as those used by Martinez et al. in order to be able to compare their fully implicit results with the semi implicit results obtained by Martinez et al.. Although the results of two computational models are in good agreement, neither of them can be applied to other operating conditions, because the models are not calibrated based on experimental results. In this research, however, the authors performed a series of column tests using intermittent irrigation of water on top of 40 cm high columns composed of ore with particles smaller than 25 mm. They obtained the shape parameters for the characteristic curve of soil-water, experimentally and calibrated their computational model based on the experimental results. The model can now be used for other operating conditions.

2. MATHEMATICAL SIMULATION OF HEAP LEACHING

Modelling of processes occurring in heap leaching is done in two stages. The first stage is simulating the movement and diffusion of solution through the bed and within the particles. This stage consists of two models, one for diffusion of solution into the particle (particle model) and the other for diffusion and movement of solution among the particles (bed model). These two models are coupled due to equality of potential at the surface of particle (interface of particles and bed) and mass flux at the surface of particle. The first stage modelling gives (a) the local values of the degree of saturation at different times, (b) the local values of diffusion coefficient and hydraulic conductivity, and (c) the local values of vertical velocity of fluid. The degree of saturation and vertical velocity are necessary for second stage modelling. The second stage modelling, simulates (a) the movement and diffusion of reagent in the bed and particles, (b) chemical reaction of reagent with reactants, (c) radial diffusion of dissolved species in the particle, and (d) vertical movement of reaction products through the bed. An ore heap is considered as a porous medium formed by particles of different sizes. The analysis is simplified assuming uniform particles in the bed. The macroscopic and microscopic structure of an ore bed are shown schematically in Figure 1.

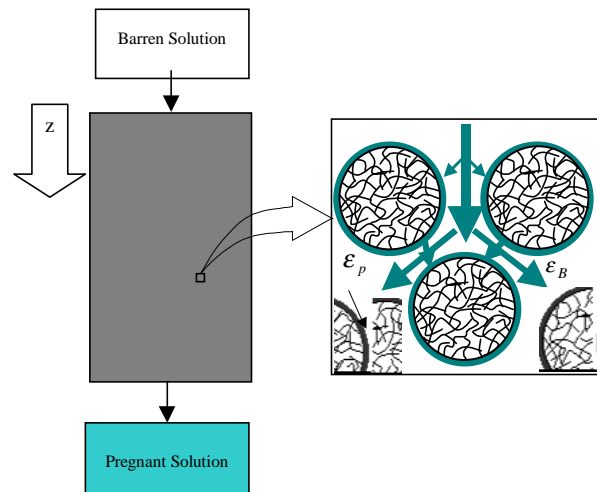


Fig. 1 Schematic of a ore heap (macroscopic and microscopic view)

The bed porosity, ϵ_B , is defined as the ratio of void space among the particles to the total volume of bed, and particle porosity, ϵ_p , is defined as the ratio of void space within the particle to the total volume of the particle. Usually, the porosity of ores that consist of relatively compact particles is lower than the porosity of the bed. Therefore, transport properties and capillary pressure of liquid among the particles will be different from the transport and capillary pressure of liquid within the particles.

2.1 Unsaturated flow of liquid through a porous bed

The mass conservation equation for unsaturated flow of a liquid through a porous medium is [7]:

$$\frac{\partial(\epsilon_l \rho_l)}{\partial t} = -\text{div} \left(\rho_l \vec{u} \right) + q_l \quad (1)$$

where, ϵ_l is liquid volumetric ratio, ρ_l liquid density, t time, \vec{u} superficial velocity vector of liquid, and q_l volumetric rate of production or consumption of liquid. The superficial velocity vector, according to Darcy's law applied to unsaturated flow, is defined as [8]:

$$\vec{u} = -K_l \vec{\text{grad}} \Phi \quad (2)$$

where, Φ is potential of liquid phase, and K_l is unsaturated hydraulic conductivity, which depends on liquid pressure due to capillary effects. Liquid potential is defined as the sum of gravity and pressure potentials [8]:

$$\Phi = h_l - z \quad (3)$$

where, z is depth from datum, and h_l liquid pressure head that is related to air pressure, p_a , and capillary pressure, p_c , as:

$$p_c = p_a - \rho_l g h_l \quad (4)$$

where, g is the gravitational acceleration. If shear stress

at interface of liquid and air is negligible, air pressure is constant and equal to atmospheric pressure and considered as reference pressure, Eq. (4) then reduces to:

$$h_l = -p_c / (\rho_l g) \quad (5)$$

Van Genuchten [8] has presented a parametric model for describing soil-water retention curves (SWRC). According to this model, the pressure head is related to effective saturation, S_e , as follows:

$$h_l = \frac{1}{\alpha} [S_e^{-1/m} - 1]^{1/n} \quad (6)$$

where, α and n are shape parameters of SWRC which are obtained from experimental data and $m=1-1/n$. The effective saturation is defined as:

$$S_e = \frac{\epsilon_l - \epsilon_r}{\epsilon - \epsilon_r} = \frac{S_l - S_r}{I - S_r} \quad (7)$$

where, ϵ is the porosity of medium, $\epsilon_l (=S_l \epsilon)$ liquid volumetric ratio, and $\epsilon_r (=S_r \epsilon)$ residual liquid volumetric ratio. S_l and S_r are liquid saturation and residual saturation respectively. ϵ_l varies between a minimum value, ϵ_r , and a maximum value, ϵ . S_l varies between S_r and unity and S_e varies between zero and one. Variation of liquid pressure with respect to liquid volumetric ratio for a sample of soil is shown in Figure 2.

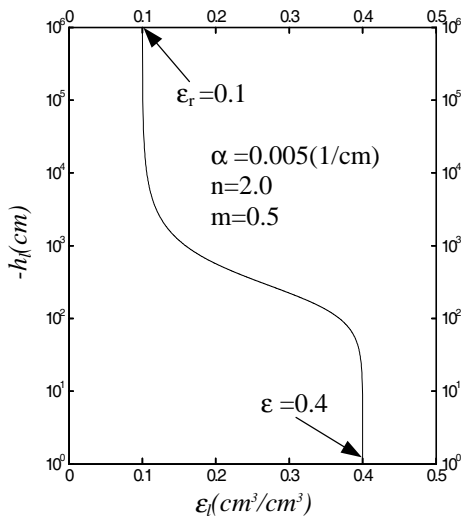


Fig. 2 A sample of soil water retention curve (SWRC)

Hydraulic conductivity of unsaturated medium is defined as:

$$K_l = K_s K_{rl} \quad (8)$$

where, K_s is saturated hydraulic conductivity and K_{rl} the relative permeability of the liquid phase. Saturated hydraulic conductivity is related to properties of liquid and porous medium as:

$$K_s = \frac{k_i \rho_l g}{\mu_l} \quad (9)$$

where, μ_l is dynamic viscosity of liquid, and k_i intrinsic permeability of the porous medium which is

independent of liquid properties and depends on structure and geometry of medium [1]:

$$k_i = \frac{d_p^2}{180} \frac{\epsilon^3}{(1-\epsilon)^2} \quad (10)$$

where, d_p is the diameter of particles forming the bed. This relation applies for a bed consisting of uniform size particles. However, it may be used for a bed consisting of non-uniform particles when the particle diameter is replaced by the effective or average diameter. Allen and Hazen [8], have selected d_{10} as the effective diameter for a bed consisting of non-uniform particles. d_{10} is the diameter of the particle, that about 10 percent of the particles are smaller than it. This diameter is determined by particle sizing analysis.

The relative permeability, K_{rl} , is defined as [9]:

$$K_{rl} = S_e^{\frac{1}{2}} \left[I - \left(I - S_e^{\frac{1}{m}} \right)^m \right]^2 \quad (11)$$

Having defined the parameters in Eq. (1), this equation can be further simplified by inserting Eq. (2) into it:

$$\frac{\partial S_l}{\partial t} = \text{div} \left(D_l \vec{\text{grad}} S_l \right) - \frac{\partial K_l}{\epsilon \partial z} + q_l / (\epsilon \rho_l) \quad (12)$$

where, D_l is the superficial diffusivity of liquid and is defined as [9]:

$$D_l = K_l \frac{\partial h_l}{\partial \epsilon_l} = \frac{(1-m)K_s}{m\alpha(\epsilon - \epsilon_r)} \times S_e^{1/2-1/m} \left[\left(1 - S_e^{1/m} \right)^{-m} + \left(1 - S_e^{1/m} \right)^m - 2 \right] \quad (13)$$

The set of equations presented in this section, constitute the governing equations for unsaturated flow of a liquid through a porous medium, which can be solved using the initial and boundary conditions for a specific problem.

2.2 Diffusion of liquid within the particle

As stated before, the particles forming the ore bed are assumed to be spherical and uniform. Lean liquor solution flows symmetrically among these particles. Therefore, liquid diffusion within the particles is one-dimensional in radial direction. As the liquid flows through the bed downwards, it diffuses into or out of the particles. When the liquid volumetric ratio at the particle outer surface is greater than that at the particle center, the diffusion will be towards the particle center, vice versa.

The mass conservation equation in the particle, according to Eq. (12), is written as:

$$\frac{\partial S_p}{\partial t} = \frac{1}{r^2} \frac{\partial}{\partial r} \left(r^2 D_p \frac{\partial S_p}{\partial r} \right) + q_{lp} / (\epsilon_p \rho_l) \quad (14)$$

where, r is radial distance, and other variables have already been defined and the subscript p refers to the particle. It should be noted that since this equation is written for a particle at a certain depth of bed, the term $\partial K_p / \partial z$ is zero. Equation (14) applies for diffusion of liquid within the particles. Diffusivity, D_p , is defined according to Eq. (13):

$$D_p = \frac{(1 - m_p) K_{sp}}{\alpha_p m_p (\epsilon_p - \epsilon_{rp})} S_{ep}^{1/2 - 1/m_p} \times \left[\left(1 - S_{ep}^{1/m_p} \right)^{-m_p} + \left(1 - S_{ep}^{1/m_p} \right)^{m_p} - 2 \right] \quad (15)$$

where, all variables have already been defined and the subscript p refers to the particle. The source or sink term, q_{lp} , is used when condensation or evaporation takes place within the particles.

Equation (14) should be solved to determine the distribution of liquid volumetric ratio or saturation within the ore particle.

To solve this equation, one initial condition and two boundary conditions are required. At the beginning of infiltration the liquid volumetric ratio within the particles is assumed to be known and uniform, thus the initial condition is:

$$S_p(r, z, 0) = S_{p0} \quad (16)$$

where, S_{p0} is the initial degree of saturation within the particle.

Because of symmetry, the gradient of degree of saturation at the center of the particle will be zero, i.e.:

$$\left. \frac{\partial S_p(r, z, t)}{\partial r} \right|_{r=0} = 0 \quad (17)$$

The second boundary condition is obtained from the equality of potential at the interface of particle and the bed (the particle surface). Since at a certain depth of the bed, the value of z in the bed and particle is the same, then:

$$h_{lp}(R, z, t) = h_{lB}(z, t) \quad (18)$$

where, h_{lp} is the liquid pressure within the particle and h_{lB} is the liquid pressure in the bed. It should be noted that in Eq. (18) the liquid volumetric ratio at the interface of particle and the bed are not necessarily the same, and therefore the initial liquid volumetric ratio in the bed and particle may be different.

2.3 Diffusion and movement of solution through the bed

It is assumed that the bed has a uniform, homogeneous and isotropic structure. The movement and diffusion of liquid is occurred in the vertical

direction towards the bottom of the bed. Then, according to the assumptions, the mass conservation equation in the bed, from Eq. (12), becomes:

$$\frac{\partial S_B}{\partial t} = \frac{\partial}{\partial z} \left(D_B \frac{\partial S_B}{\partial z} \right) - \frac{\partial K_B}{\epsilon_B \partial z} + q_{lB} / (\epsilon_B \rho_l) \quad (19)$$

where, z is the depth, and other variables have already been defined and subscript B refers to the bed. This equation applies for the diffusion and movement of liquid among the particles. The hydraulic conductivity of the bed, K_B , according to Eqs. (8) and (11), is determined as:

$$K_B = K_{sB} S_{eB}^2 \left[1 - \left(1 - S_{eB}^{1/m_B} \right)^{m_B} \right] \quad (20)$$

and the diffusivity, D_B , from Eq. (13) becomes:

$$D_B = \frac{(1 - m_B) K_{sB}}{\alpha_B m_B (\epsilon_B - \epsilon_{rB})} S_{eB}^{1/2 - 1/m_B} \times \left[\left(1 - S_{eB}^{1/m_B} \right)^{-m_B} + \left(1 - S_{eB}^{1/m_B} \right)^{m_B} - 2 \right] \quad (21)$$

The source or sink term, q_{lB} , represents the mass diffused into or out of the particles as well as the mass condensed or evaporated among the particles. If the phase change among the particles is negligible, coupling the bed and particles is done by the source or sink term, q_{lB} . Considering the available particle surface in a volume element of bed, the source (or sink) term is determined as:

$$q_{lB} = -3 \frac{\epsilon_p}{R} \rho_l (1 - \epsilon_B) \left(D_p \frac{\partial S_p}{\partial r} \right)_{r=R} \quad (22)$$

where R , is the radius of particle.

According to Eqs. (2), (3), and (13), the vertical velocity of liquid in the bed is determined as:

$$u = -\epsilon_B D_B \frac{\partial S_B}{\partial z} + K_B \quad (23)$$

Equation (19) should be solved to determine the distribution of liquid volumetric ratio or saturation within the bed. To solve this equation, one initial condition and two boundary conditions are required. At the beginning of infiltration the liquid volumetric ratio within the bed is assumed to be known and uniform, thus the initial condition is:

$$S_B(z, 0) = S_{B0} \quad (24)$$

where, S_{B0} is the initial degree of saturation of the bed.

The first boundary condition is defined from mass flux at the top surface of the bed. Liquid applied to the bed at this surface flows through the bed due to gravity and capillary forces, then:

$$u(t) = -\epsilon_B D_B \frac{\partial S_B}{\partial z} + K_B \Big|_{z=0} \quad (25)$$

where, $u(t)$ is the superficial velocity of liquid applied to the top surface of bed that is a constant value, u_{in} , when the liquid infiltration is continuous, and is a step function of time when the infiltration is intermittent:

$$u(t) = \begin{cases} u_{in} & \text{at washing period} \\ 0 & \text{at rest period} \end{cases} \quad (26)$$

It is assumed that liquid exits from the bottom of the bed and enters to a medium of negligible resistance with atmospheric pressure. Then, the gradient of liquid volumetric ratio or degree of saturation at the bottom is zero:

$$\left. \frac{\partial S_B(z,t)}{\partial z} \right|_{z=H} = 0 \quad (27)$$

where, H is the height of the bed.

Solving Eqs. (14) and (19) together with initial and boundary conditions gives the distribution of liquid volumetric ratio in the particle and the bed. Equation (23) is then used to work out the vertical velocity of liquid in the bed.

3. COMPUTATIONAL PROCEDURE

The partial differential equations with variable coefficients, governing liquid flow in the bed and particles (Eqs. (14) and (19)), can not be solved analytically. They are solved using computational techniques. To solve these equations, a uniform spherical mesh is fitted to the particle and a uniform and one-dimensional mesh to the bed. Using fully implicit finite difference method, the governing partial differential equations are discretized and converted to a set of algebraic equations. The initial values of pressure head, hydraulic conductivity and diffusivity are determined using the initial liquid volumetric ratio. The resulting sets of algebraic equations are solved using Thomas Algorithm [10] and iterative method to get the corresponding values at the next time increment. The maximum of relative errors in the degree of saturation of the bed and particles is compared with the maximum allowable error in the computational method. The calculations are repeated until the maximum relative error becomes less than 10^{-6} . The number of mesh points in the particle and the bed depends on the particle radius and bed height. The time increment is set according to the total time of process. The flowchart of computer program is shown in Figure 3.

4. COLUMN TESTS

In order to ensure the accuracy of numerical results, a number of column tests were carried out using oxide ore in the Sarcheshmeh Copper Complex. The oxide

ore used for column testes was taken from the West Dump of the oxide ores, which is currently being used for heap leaching. A sample of 1600 kg of oxide ores was chosen randomly and mixed thoroughly, from that a smaller sample of 130 kg was selected and the pieces greater than 25 mm were separated. The remainder ore particles were splitted several times and finally a sample of 10.8 kg for sizing analysis and a sample of 1.819 kg for moisture measurement were selected. The results of sizing analysis and moisture measurement are represented in Tables 1 and 2 respectively. Table 1 indicates that about 25% of the particles have diameters smaller than 1.0 mm and about 30% of the particles have diameters smaller than 1.4 mm. Therefore, effective diameter of $d_{25}=1.0$ mm and $d_{30}=1.4$ mm were chosen. Three columns of transparent material (Plexiglas) having inner diameter of 8.8 cm and height of 50 cm were used. These columns are called G1, G2 and G3. The schematic diagram of a test column is shown in Figure 4. The specifications of columns are shown in Table 3. The height and diameter of the columns are selected in a way that the end effects are negligible [7].

The periodic flow rate of infiltration is fixed at $1 \text{ cm}^3/\text{min}$ which is equivalent to $10 \text{ litre}/\text{m}^2\text{hr}$. The period of infiltration is 6 hrs for the total duration of 72 hrs. A peristaltic pump provides the entrance volume flow rate, and the exit flow rate is measured manually during the test duration.

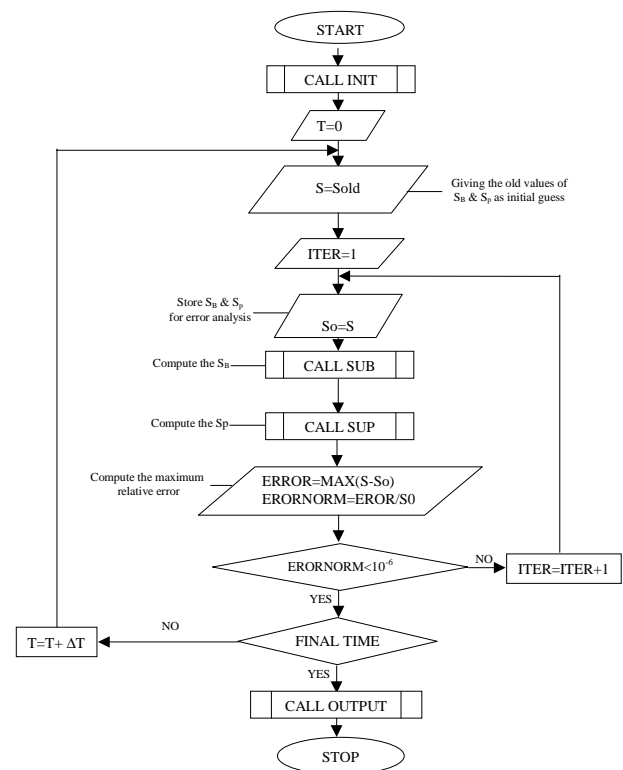


Fig. 3 Flow chart of computer program

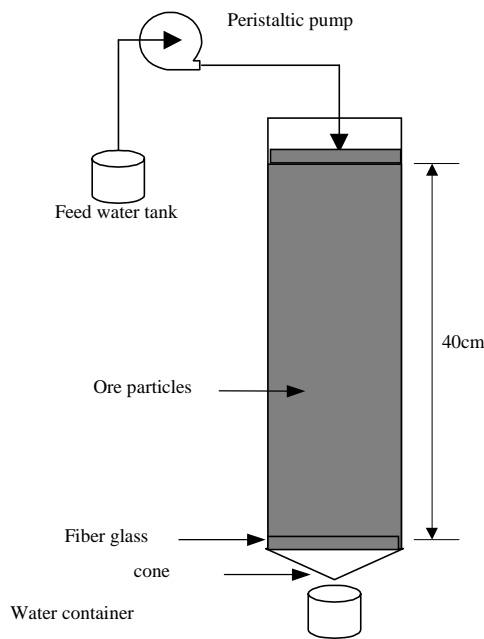


Fig. 4 Schematic diagram of test column

Table 1 Analysis of size particles of ore sample

Mesh size [mm]	Average diameter [mm]	Weight [gr]	Percent [%]
15.8-25	20.4	882.4	8.2
6.7-15.8	11.3	2800.8	25.9
3.3-6.7	5.0	2014.4	18.7
1.7-3.3	2.5	1458.7	13.5
1.2-1.7	1.4	502.9	4.6
0.8-1.2	1.0	645.9	6.0
0.4-0.8	0.6	874.2	8.1
0.2-0.4	0.3	704.0	6.5
-0.21	-	916.2	8.5

Table 2 Results of moisture measurement

Weight of ore sample before drying	Weight of ore sample after drying	Weight of evaporated moisture	Ratio of evaporated moisture
1819 gr	1798 gr	21 gr	% 1.15

Table 3 Specifications of test columns

	G1	G2	G3
Particles diameter	-25 mm	0.8-1.2 mm	1.2-1.7 mm
Ore weight	3900 gr	2980 gr	2910 gr
Height of ore bed	40 cm	40 cm	40 cm
Bulk density of ore	1.6 gr/cm ³	1.26 gr/cm ³	1.26 gr/cm ³
Bed porosity	0.41	0.55	0.56

5. RESULTS AND DISCUSSION

Computational investigation of unsaturated flow of liquid in heap leaching has been performed using experimental information and reasonable assumptions. For instance, the residual liquid volumetric ratio in the ores is relatively high [11], but a smaller value of residual liquid volumetric ratio is assumed for the ore

bed, because the bed has a larger porosity than the ore particles. The computer program was run using different values of α , n and ϵ_r . It has been noticed that the computational results conform with the experimental ones when the values of α , n and ϵ_r for the particles and the bed are as follows:

$$\begin{aligned} \text{Particle: } & \alpha=1 \quad n=1.2 \quad S_r=0.5 \\ \text{Bed: } & \alpha=3 \quad n=1.39 \quad S_r=0.01 \end{aligned}$$

The above values have been applied to the computer program, based on that, the SWRC of the bed and the particles have been shown in Figure 5. The SWRCs are plotted using the Mualem model defined in Eq. (4) [9]. The curves are used to evaluate the liquid pressure versus the degree of saturation.

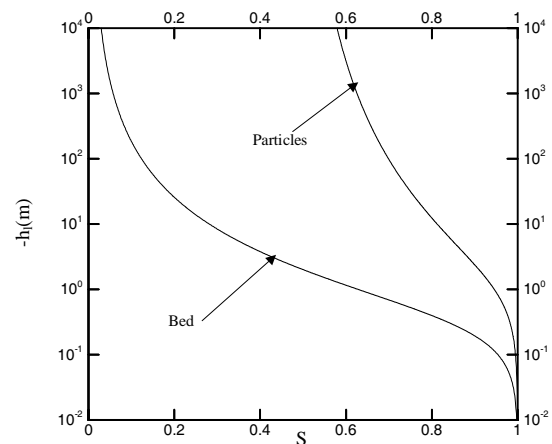


Fig. 5 Variations of liquid pressure in bed and particles with respect to degree of saturation

The hydraulic conductivity and liquid diffusivity depend on intrinsic permeability, which is a function of porous medium structure (Eq. (8)). The intrinsic permeability changes in the range of 3×10^{-12} to $3 \times 10^{-7} \text{ m}^2$ when the bed porosity varies between 0.3 and 0.5 for the particle diameter of 0.1 mm to 10 mm. The hydraulic conductivity and diffusivity in the above range are shown in Figures 6 and 7 respectively. It can be seen that both parameters depend strongly on the degree of saturation. The intrinsic permeability in ore beds is roughly 10^{-9} m^2 , although it may vary locally due to non-homogeneity of the bed. The intrinsic permeability of particles is more uncertain, but as an order of magnitude, it may be considered to be about 10^{-15} m^2 [5]. The intrinsic permeability of the bed is calculated using Eq. (10).

The numerical results are compared with the results obtained from the column tests in order to calibrate the numerical model. The model can then be applied to any operating conditions. Figures 8 and 9 compare the numerical results with the results obtained from the column tests for ores having particles smaller than 25 mm and about 1 mm respectively. It is observed that the results are in good agreement and the discrepancy is about 10 percent. Based on this agreement, an effective diameter of $d_{25}=1 \text{ mm}$ has been adopted for the ore having particles smaller than 25 mm.

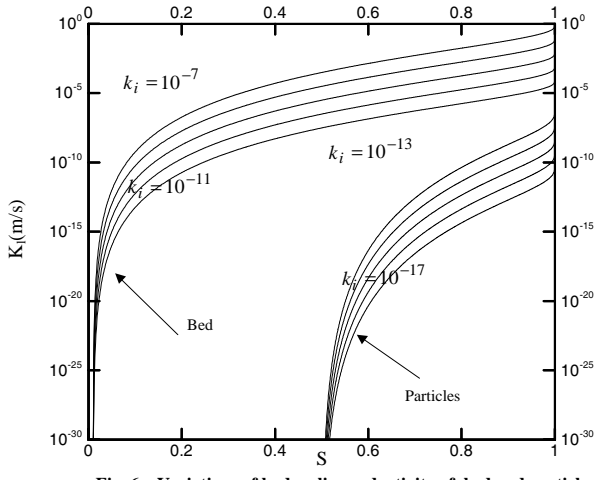


Fig. 6 Variations of hydraulic conductivity of bed and particles with respect to degree of saturation

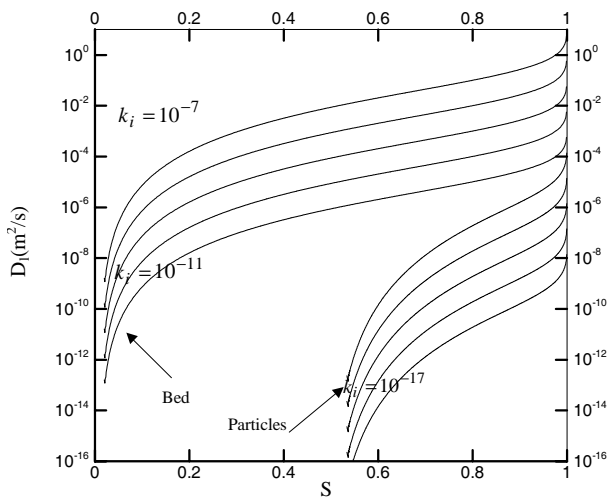


Fig. 7 Variations of diffusivity of bed and particles with respect to degree of saturation

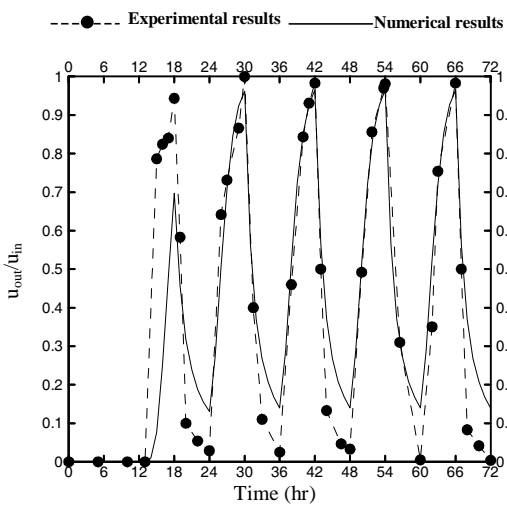


Fig. 8 Variations of volumetric flow rate ratio with respect to time for column G1

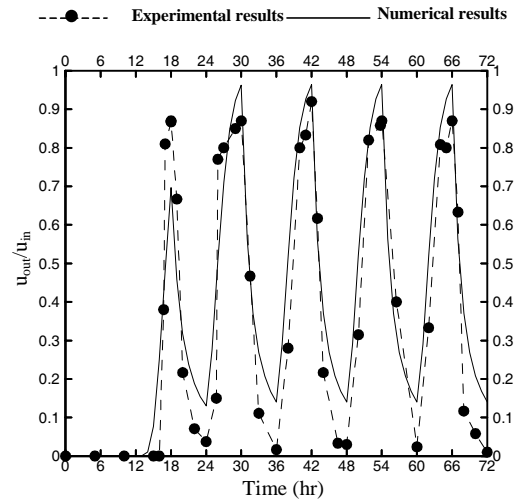


Fig. 9 Variations of volumetric flow rate ratio with respect to time for column G2

The time required to reach steady state and the degree of saturation in the bed and particles at steady state conditions are important parameters for the ore heaps. When the steady state conditions prevail, the hydraulic conductivity of the bed will be equal to the superficial infiltration velocity, this is because, at steady state conditions the degree of saturation will be uniform throughout the bed. The same condition occurs in the particles. Consequently, the mass flow rate at inlet and outlet will be the same.

The effect of important parameters on the distribution of the degree of saturation of the bed and particles as well as the bed exit mass flow rate has been considered under different operating conditions. In this computational study, the parameters their effect on the degree of saturation has been studied are the bed intrinsic permeability, infiltration rate, and the bed height. To make sure the numerical results are independent of the mesh size, the computations have been performed for different mesh sizes. The results of a typical survey for 5 different mesh sizes have been indicated in Figure 10. It has been observed that the ratio of exit to entrance mass flow rate with respect to time does not change considerably when the numbers of grid points (N_z) are 400 or 500. To be more specific, the number of grid points has been taken to be 500. It is worth mentioning that, in the calibration procedure, the same mesh size (bed height/number of grids) has been used for the numerical calculations. The independent mesh size has then been chosen such that having 500 grid points in a bed of the height of 5 m. This proportion has been applied to all other computations.

Figure 11 indicates the variations of the ratio of mass flow rate ratio with respect to time for 4 different bed heights, when the intrinsic permeability has a value of $k_i = 10^{-8}$. As can be predicted, the time required for the liquid to reach the bottom of the bed increases as the bed height is increased and the steady conditions occur at a later time. Therefore, in intermittent infiltration a longer period can be taken into account for higher beds.

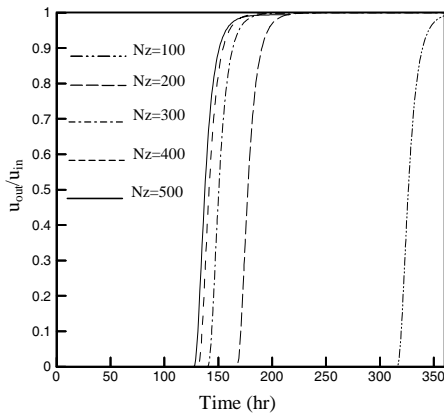


Fig. 10 Effect of mesh size on volumetric flow rate ratio with respect to time for $H=5m$

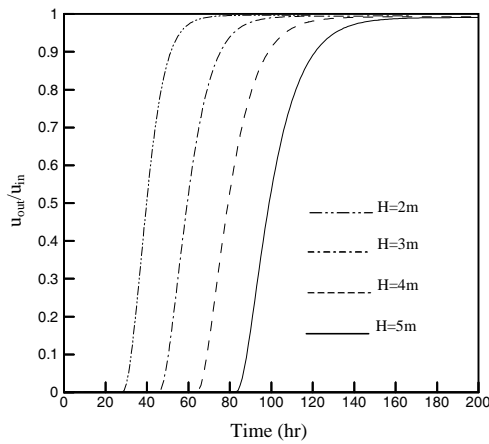


Fig. 11 Effect of bed height on volumetric flow rate ratio with respect to time for $k_i=10^{-8}$

Figure 12 shows the variations of the ratio of mass flow rates with respect to time for 4 different k_i when the bed height is fixed at $1 m$. It is observed that, the time required for the liquid to reach the bottom of bed decreases as k_i is increased and the steady state condition occurs sooner.

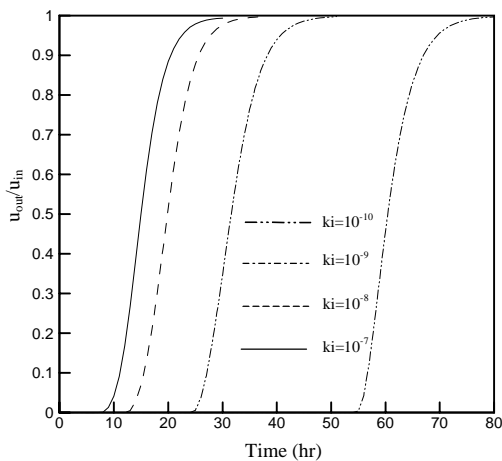


Fig. 12 Effect of intrinsic permeability on volumetric flow rate ratio with respect to time for $H=1 m$

Figure 13 indicates the variations of the time required to reach the steady state condition, τ , with respect to infiltration rate, u_s , for 3 different k_i when the bed height is fixed at $H=5 m$. The figure shows when u_s is small, the steady state condition is established very late. On the other hand, as u_s is increased, τ is shortened very rapidly and approaches to a relatively constant value at high infiltration rate. It is also noticed that the lower k_i , the higher τ .

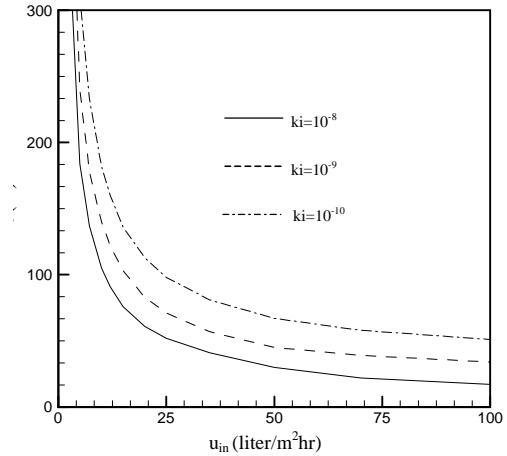


Fig. 13 Effect of intrinsic permeability on time required to reach steady state condition with respect to infiltration rate for $H=5 m$

Figure 14 shows the variations of the degree of saturation of the bed in steady state condition with respect to u_s , for 3 different k_i when the bed height is fixed at $H=5 m$. The figure shows that for the infiltration rate in the range of $0 < u_s < 10 \text{ litre/m}^2\text{hr}$ the degree of saturation of bed in steady state condition increases rapidly when u_s is increased, and for higher values of u_s the slope of the curve becomes very small and the degree of saturation approaches to a constant value. It is further noticed that for lower k_i a higher degree of saturation in steady state condition is achieved.

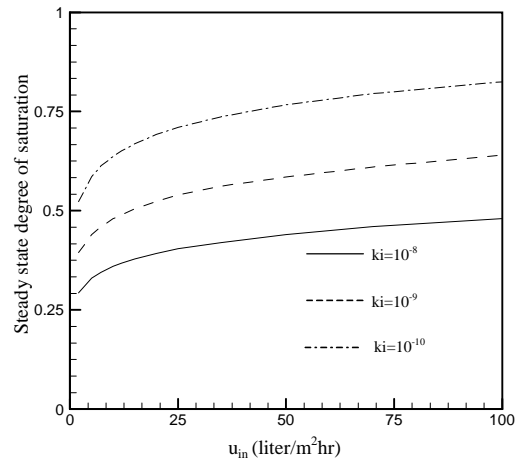


Fig. 14 Effect of intrinsic permeability on steady state degree of saturation with respect to infiltration rate for $H=5 m$

It should be mentioned that the leaching processes take place in the liquid within the bed and particle pores, therefore the distribution of liquid volumetric ratio should be known for the bed and particle at any increment of time.

Figure 15 shows the variations of the degree of saturation at the particle center with respect to time at 3 different depths when $u_s=7.2 \text{ litre/m}^2\text{hr}$ and $H=5 \text{ m}$. This variation is shown for 2 different k_i . It is noticed that at the top of the bed ($z=0$) the particle's degree of saturation increases rapidly and reaches to the steady state condition quickly, while at higher depths ($z=2.5, 5 \text{ m}$) this behavior takes place at a later time. This is because of the delay in wetting the bed at higher depths. It is also observed that the lower the bed intrinsic permeability, the higher the degree of saturation at the particle center. The reasoning for this observation is that when the intrinsic permeability is reduced, the liquid velocity through the bed is decreased and the bed's degree of saturation is increased. To study the effect of intermittent infiltration on the degree of saturation, the bed height, the infiltration rate and the period are specified as 5 m , $7.2 \text{ litre/m}^2\text{hr}$ and 1 day respectively.

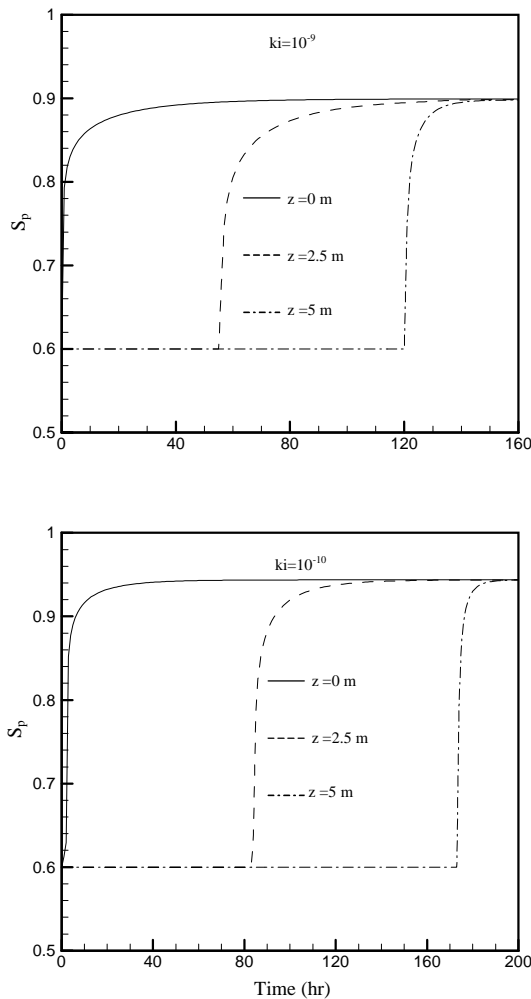


Fig. 15 Variations of degree of saturation at the particle center with respect to time at top, middle and bottom of the bed

Figure 16 indicates the variations of the degree of saturation of the bed with respect to the bed's depth at different time intervals. The figure shows that the distribution of the degree of saturation can be studied in two different stages. The first stage refers to the early days (10 days) and the second stage refers to the later days (10-20 days). In the first stage, the liquid penetrates to deeper depths of the bed, makes the deeper depths wet and results in large variations in the degree of saturation. In the second stage, the bed's degree of saturation changes between two limiting values and the variations are much less than the first stage. In other words, the profiles of the degree of saturation of the bed are repeated in each period. This behavior is highly depending on the bed height, the bed intrinsic permeability, infiltration period and infiltration rate. That means, the first stage (defined as the transient time) and also the limiting values of the degree of saturation in the second stage depend on the above parameters.

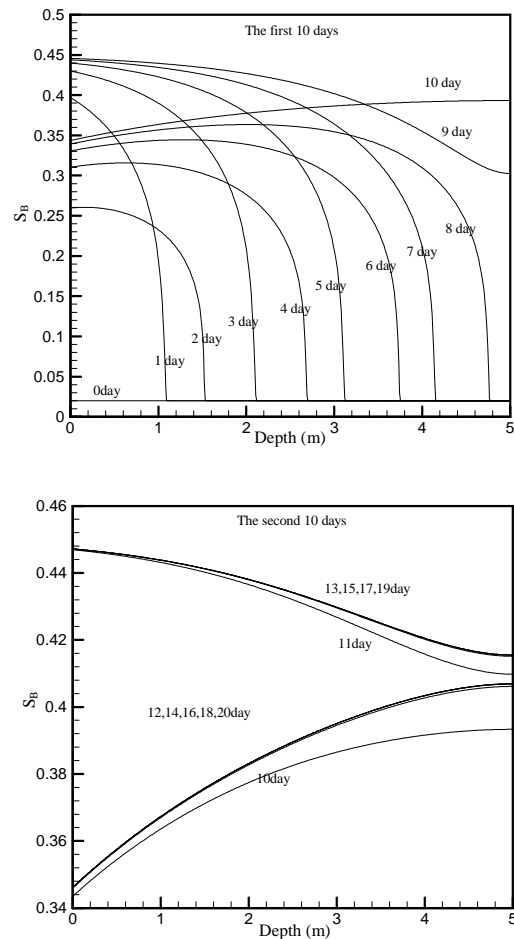


Fig. 16 Variations of degree of saturation in the bed at various time increments

Figure 17 indicates the variations of the degree of saturation with respect to time at the top and bottom of the bed. It can be observed that the fluctuation of the degree of saturation at the top of the bed starts immediately and the amplitude of the fluctuations becomes invariable after a few days. The fluctuation

of the degree of saturation at the bottom of the bed starts when the liquid reaches there, and the amplitude of the fluctuations becomes invariant very quickly. The magnitude of the fluctuation amplitude at the bottom of the bed is lower than that at the top of the bed.

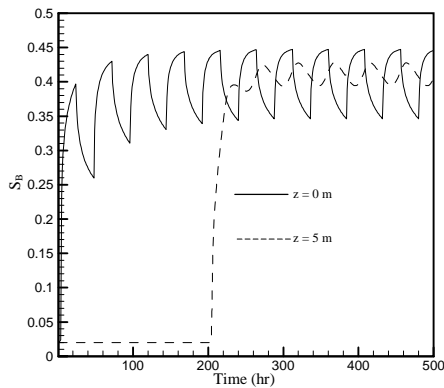


Fig. 17 Variations of degree of saturation at top and bottom of the bed with respect to time for $H=5\text{ m}$

Figure 18 indicates the variations of the degree of saturation with respect to time at the top and bottom of the bed for three intrinsic permeabilities of the bed. It is realized that the amplitude of the fluctuations of the degree of saturation is reduced as the permeability increases. The amplitude eventually approaches to a constant value, which depends on the permeability. The fluctuations at the bottom of the bed start at a later time and the magnitude of the amplitude is lower than that at the top of the bed.

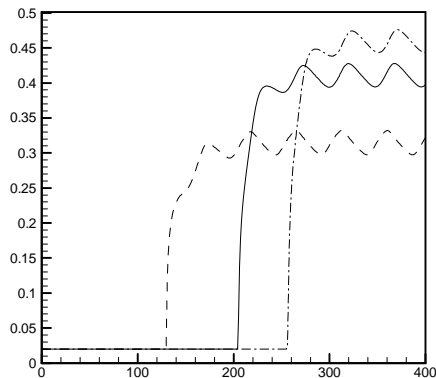
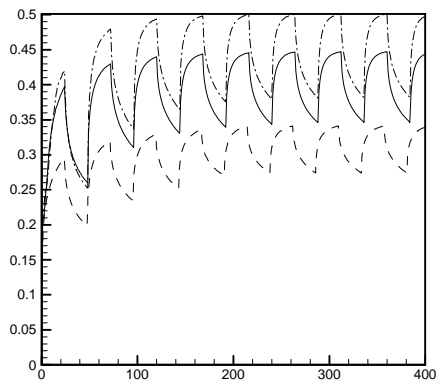


Fig. 18 Effect of intrinsic permeability on degree of saturation at top and bottom of the bed with respect to time for $H=5\text{ m}$

As mentioned before, the degree of saturation is not only a function of intrinsic permeability, but also changes with respect to infiltration period.

Figure 19 indicates the variations of the degree of saturation with respect to time at the top and bottom of the bed for two periods. It is observed that the amplitude of fluctuations increases as the period is increased.

From the information of the degree of saturation in the bed, one can figure out the void space available for airflow among the ore particles, which is of great importance in leaching of sulfide ores.

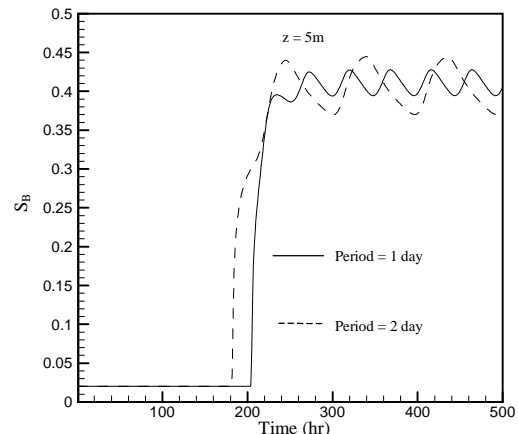
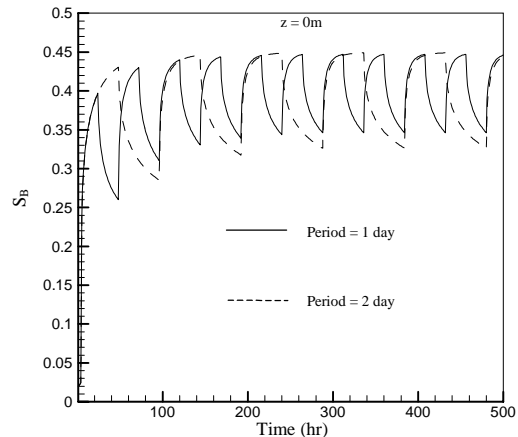


Fig. 19 Effect of infiltration period on degree of saturation at top and bottom of the bed with respect to time for $H=5\text{ m}$

6. CONCLUSION

Unsaturated flow of liquid through the ore bed depends strongly on the bed and ore particles characteristic curves. Periodic infiltration results in quasi-steady state in which the profiles of degree of saturation in the bed vary between two limiting values. The fluctuations of the degree of saturation depend not only on period, but also vary with intrinsic permeability and the depth in the bed. It is reduced when the intrinsic permeability or the depth is increased. The degree of saturation is increased when the infiltration period is increased.

The accuracy of numerical results obtained from this modelling depends on how reliable the data of characteristic curves of the bed and particles are. Having such reliable data, one can predict how periodic infiltration affects the macroscopic and microscopic movement of reagent and dissolved species through the bed. Furthermore, it can be seen, if an almost constant concentration of the desired specie in an acceptable duration can be achieved, using periodic infiltration.

7. ACKNOWLEDGEMENT

The authors wish to thank the Research and Development Office of the Sarcheshmeh Copper Complex for their support regarding this research.

8. REFERENCES

- [1] D.A. Nield and A. Bejan, *Convection in Porous Media*, Springer, New York, 1999.
- [2] G.A. Sheikhzadeh, M.A. Mehrabian, S.H. Mansouri and A. Sarrafi, Investigation of ore bed specifications and liquid flow in heap leaching, Proc. of the 7th National Iranian Chemical Engineering Congress, University of Teheran, Vol. 4, pp. 56-63, 2002.
- [3] R.W. Bartlett, *Solution Mining: Leach and Fluid Recovery of Materials*, Gordon and Breach Science Publishers, Reading, 1992.
- [4] J.F. Rauld, R. Montealegre, P. Schmidt and E. Domic, T.L. Leaching Process: A Phenomenological Model for Oxide Copper Ores Treatment, Hydrometallurgical Reactor Design and Kinetics, TMS-AIME Meeting, New Orleans, 1986.
- [5] L. Martinez, L. Moreno and J.M. Casas, Modelling of intermittent irrigation in leaching heaps, *Electrorefining and Hydrometallurgy of Copper*, Vol. 3, 1995.
- [6] G.A. Sheikhzadeh, M.A. Mehrabian, S.H. Mansouri and A. Sarrafi, Simulation of unsaturated flow of liquid with periodic infiltration in a bed of porous ore particles, Proc. of the 11th Iranian Annual Mechanical Engineering Conference, Ferdowsi University of Mashhad, Vol. 1, pp. 43-50, 2003.
- [7] F.A.L. Dullien, *Porous Media: Fluid Transport and Pore Structure*, Academic Press Inc., New York, 1979.
- [8] J. Ghazanshahi, *Soil Physics*, Tehran University Press, 1995.
- [9] T. Van Genuchten, A closed form equation for predicting the hydraulic conductivity of unsaturated soils, *Soil Sci. Soc. Am.*, Vol. 44, pp. 892-898, 1980.
- [10] S.V. Patankar, *Numerical Heat Transfer and Fluid Flow*, Washington, McGraw-Hill, 1980.
- [11] W.A. Kennedy and J.R. Stahl, Fluid retention in leach dumps by capillary action, Proc. of the Solution Mining Symposium, 103rd AIME Annual Meeting, Dallas, Texas, Chapter 8, pp. 99-128, 1974.

PRIMJENA NUMERIČKIH METODA U SIMULACIJI NESTACIONARNOG TOKA TEKUĆINA KROZ POROZNI MEDIJ OD POROZNIH ČESTICA RUDE

SAŽETAK

Proučava se numerički i eksperimentalno nezasićeni tok tekućina na podlozi jednolikih i oblikih čestica rude. Sačinjen je nepravilan i dvodimenzionalni model koji se bazira na jednadžbama očuvanja mase tekućine na podlozi i u česticama. Jednadžbe modela rješavaju se koristeći potpuno implicitnu metodu konačne razlike koja daje distribuciju stupnja zasićenosti u česticama i na podlozi kao i vertikalnu brzinu toka na podlozi, također i djelovanje periodičke infiltracije u gore spomenutim distribucijama. Da bi se kalibrirali modeli proračuna napravljeno je nekoliko testova koristeći periodičku infiltraciju vode na 40 cm visokim stupovima od kovine čija je veličina čestica bila manja od 25 mm. Numerička analiza pokazuje da (a) rezultati dobiveni numeričkim modeliranjem u istim radnim uvjetima kao i testovi na stupovima slažu se s onima dobivenim eksperimentalnom metodom, (b) stupanj zasićenosti podloge i vrijeme potrebno da se postignu uvjeti stabilnog stanja ovise o dotoku vode kao i o intrinzičnoj propusnosti podloge i (c) fluktuacije brzine i fluktuacije stupnja zasićenosti u podlozi ovise o dotoku vode, periodu infiltracije, visini i intrinzičnoj propusnosti podloge.

Ključne riječi: modeliranje, nestacionarni tok tekućina, porozni medij, stupčani test.